

A Compact High-Sensitivity 2-Transistor Radiation Sensor Array

Qianying Tang Saurabh Kumar Chris H. Kim

Department of Electrical & Computer Engineering,
University of Minnesota
200 Union Street SE, Minneapolis, MN 55455, USA
tangx280@umn.edu

David E. Fulkerson

Independent Consultant, Minneapolis, USA

Abstract—A compact 2 Transistor (2T) radiation sensor with a tunable measurement sensitivity was implemented in a 65nm LP bulk process. Alpha radiation tests show a 117X higher cross-section area per cell for the proposed sensor as compared to a 6T SRAM test structure. The critical Linear Energy Transfer (LET) of the proposed 2T sensor was estimated to be 3.4x-4.2x lower than that of an inverter cell or SRAM cell for supply voltages 0.75V to 1.5V. The proposed sensor can facilitate the development of radiation models and hardening techniques by enabling a statistically significant number of events from a small silicon area using inexpensive radiation sources.

Index Terms—radiation sensor, soft error, alpha particle, 2T sensor, SRAM, inverter chain.

I. INTRODUCTION

Recent studies have shown that Soft Error Rate (SER) per memory bit is steadily decreasing with technology scaling due to the commensurate reduction in junction area [1]. Furthermore, SER in FinFET technologies is 5-10x lower than SER in planar technologies due to the smaller geometrical contact area between the diffusion and substrate regions [2], [3]. As a result, collecting statistically significant amount of SER test data in advanced technologies such as FinFET or FDSOI has become a challenging task, requiring a large number of test circuits exposed to sophisticated radiation sources for long periods of time. Extracting model parameters from a limited number of SEU, MBU, and SET events results in model inaccuracies. Extrapolating SER based on data collected at low supply voltages can lead to unrealistic SER projections.

To overcome these limitations, we present a compact 2 Transistor (2T) radiation sensor array with an unusually high sensitivity to radiation strikes. The new sensor circuit has a critical charge (Q_{crit}) that is more than 10 times smaller compared to a 6T SRAM. This is achieved by eliminating the restore current and minimizing the node capacitance. Alpha particle experiments show that the proposed 2T sensor can detect many strikes that would have otherwise gone undetected using a standard 6T SRAM test structure. The higher sensitivity to particle strikes and dense area makes the proposed 2T sensor an effective tool for performing detailed radiation studies.

II. 2T SENSOR STRUCTURE

SEUs or SETs occur when the collected charge (Q_{coll}) generated by a particle strike is greater than the Q_{crit} of the circuit node. Q_{crit} is determined by several circuit parameters such as node capacitance, supply voltage, restore current, switching threshold, and circuit topology. In particular, restore current prevents the cell voltage from being disturbed by continuously replenishing the charge loss. This can be seen in Fig. 1(a) where the SET pulse shape is determined by the amount of charge generated by a strike as well as the magnitude of the restore current. Similarly, in a 6T SRAM cell shown in Fig. 1(b), the restore current along with the cross-coupled feedback loop reinforces the data and thereby reducing the chances of an upset. Based on this observation, we propose a two-transistor (2T) structure shown in Fig. 1(c) with an extremely high sensitivity to radiation strikes. As compared to an inverter chain or an SRAM cell, the 2T sensor has a significantly lower Q_{crit} since (1) the restore current is eliminated, (2) the node capacitance is minimized. The 2T sensor cell consists of a PMOS write transistor and an NMOS

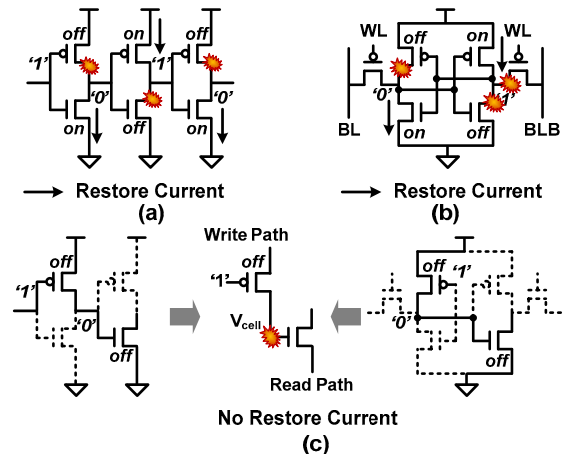


Fig. 1. Particle strike induced soft errors are rare in (a) logic gates and (b) SRAM cells because of the strong restore current. (c) The proposed 2T sensor achieves a higher sensitivity to radiation strikes by eliminating the restore current, minimizing the node capacitance, and allowing the storage node voltage to gradually decay with time.

read transistor. During irradiation mode, the sensitive node voltage V_{cell} is initialized and then left floating by turning off the write PMOS transistor. This way, a particle strike can easily disrupt V_{cell} .

The circuit diagram of a 32x32 sensor array is shown in Fig. 2. Column decoders are used for decoupled write and read operations. The column voltage determined by the selected 2T cell value is compared with an external reference voltage V_{REF} to determine the cell status. Similar to a DRAM cell, leakage currents surrounding the sensitive node causes V_{cell} to gradually discharge or charge depending on the initial voltage written to the cell. In order to separate retention time induced errors from radiation induced errors, the cell data must be read out before V_{cell} rises above or falls below the threshold. Also V_{REF} is carefully chosen to ensure that the data '1' and '0' voltage margins shown in Fig. 2 (right) are symmetric around V_{REF} .

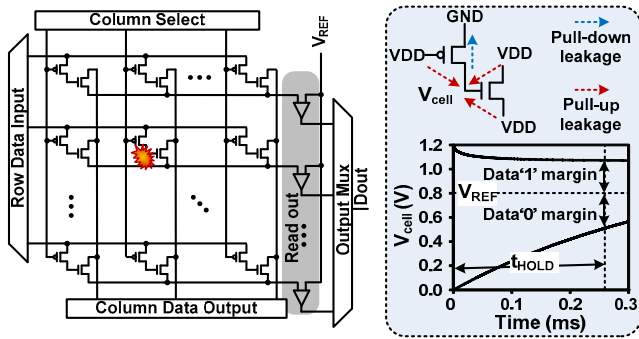


Fig. 3. Proposed 2T sensor array for detecting SEU with high sensitivity. Voltage stored inside the cell (V_{cell}) varies with time and leakage current.

III. ALPHA TEST RESULTS

The overall experiment flow is shown in Fig. 3. Although it is known that the storage node is more sensitive to radiation effect when the junction is reverse-biased (written with a data '0'), for completeness, a checkerboard pattern is written to the sensor array to investigate all possible failures. The test sequence is composed of two phases; pre-calibration phase

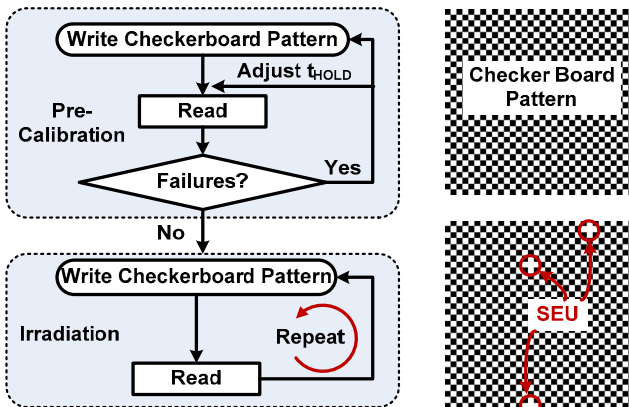


Fig. 4. Overall test sequence for the 2T sensor array. The array pattern is compared with the initial checkerboard pattern to identify particle strike induced SEUs and MBUs.

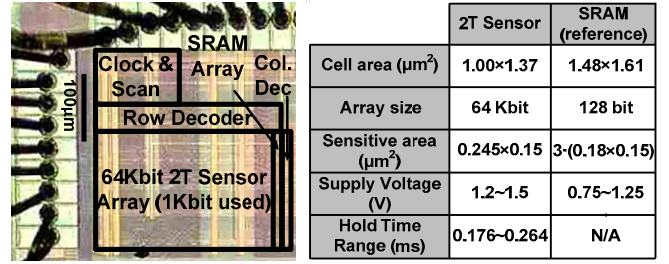


Fig. 2. 65nm test chip with proposed 2T radiation sensor array and reference SRAM cells for comparison.

and irradiation phase. During pre-calibration phase, the checkerboard pattern is written to the sensor array and subsequently, the cell data is read out after a hold time t_{HOLD} to check for any retention errors. t_{HOLD} is gradually decreased until retention errors are no longer present. To make sure no intrinsic failures occur, t_{HOLD} is selected such that a certain data margin is withheld when the cells are read out. During the irradiation phase, the array data is initialized and read out repeatedly using the specific t_{HOLD} interval found in the pre-calibration phase. SER is calculated by comparing the array pattern containing errors with the initial checkerboard pattern. The 2T sensor array chip was fabricated in a 1.2V 65nm LP bulk process. The die microphotograph and chip specifications are shown in Fig. 4. Although the total array size is 64Kbit, only 1Kbit cells were tested due to the limited number of IO pins and the lack of high-speed testing equipment. A small number of reference SRAM cells were implemented in the same chip for comparison purposes.

Even though the 2T sensor provides a very high sensitivity to single event effects, characterizing SER using a button source (e.g. Americium, Thorium) is still timing consuming. So instead, we performed radiation testing using an alpha particle accelerator housed in the Characterization Facility at the University of Minnesota shown in Fig. 5. Alpha particles were generated by a MAS 1700 pelletron tandem ion accelerator. Test chips were placed inside an end-station vacuum chamber with a controllable angle rotation. The particle energy used in our experiment was fixed at 3.8 MeV. Another commonly reported beam parameter is Linear Energy Transfer (LET) which corresponds to the energy deposited per unit length along the ion penetration track of a



Fig. 5. Particle accelerator used for radiation testing (Source: University of Minnesota Characterization Facility)

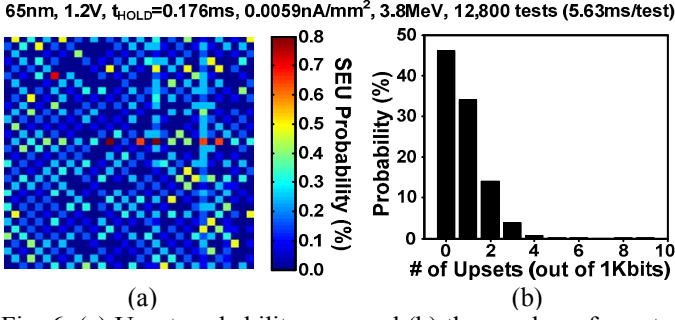


Fig. 6. (a) Upset probability map and (b) the number of upsets measured from a 1Kbit 2T sensor array.

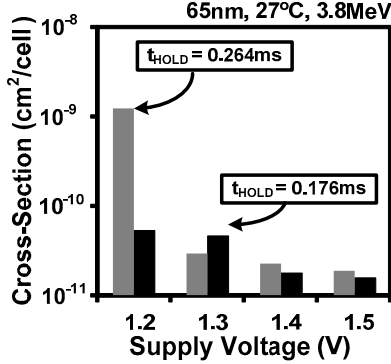


Fig. 7. Cross-section versus supply voltage for 2T sensor array measured under two different retention times.

given material. The LET used in this experiment is estimated to be $0.736\text{MeV}\cdot\text{cm}^2/\text{mg}$ using the NIST ASTAR calculator [3].

SER map of a 1Kbit array measured for 12,800 consecutive 5.63ms exposure cycles is shown in Fig. 6(a). The per-cell upset probability ranges from 0% to 0.8% under a nominal supply voltage of 1.2V. The number of ‘0’-to-‘1’ upsets is significantly higher than that of ‘1’-to-‘0’ upsets which verifies that p-n junctions under a reverse bias are vulnerable to radiation effects. Fig. 6(b) shows that upsets occur in more than 50% of the cells indicating that in most locations, the 0’-to-‘1’ upset happened at least once throughout the 12,800 exposure cycles.

Fig. 7 shows that the cross-section increases from $1.86\text{E-}11\text{ cm}^2/\text{cell}$ to $1.22\text{E-}9\text{ cm}^2/\text{cell}$ as the supply voltage is lowered from 1.5V to 1.2V for a t_{HOLD} of 0.264ms. Measurement results for a t_{HOLD} of 0.176ms show a similar trend. Fig. 8(a) illustrates the relationship between sensor cell cross-section and t_{HOLD} . The cross-section increases from $5.32\text{E-}11\text{ cm}^2/\text{cell}$ to $1.25\text{E-}9\text{ cm}^2/\text{cell}$ as the hold interval t_{HOLD} is increased from 0.176ms to 0.264ms. As shown in Fig. 8(b), with a larger hold interval, the data ‘0’ margin decreases due to leakage current which gradually pulls up the node voltage. Also, a longer exposure time further degrades the data margin resulting in an increased cross-section. The measured data in Fig. 9 confirms that cross-sections of the proposed 2T structure is proportional to radiation flux. For comparison, we measured the SER of a 128 bit 6T SRAM array implemented in the same chip. Due to rare occurrence of SRAM SEU at the nominal 1.2V supply voltage, the SRAM

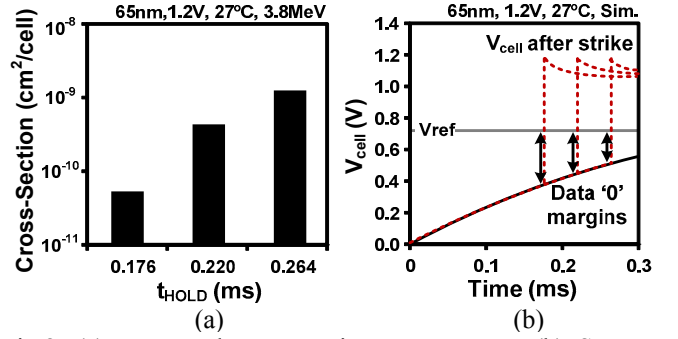


Fig. 8. (a) Measured cross-section versus t_{HOLD} (b) Storage node voltage versus time illustrating gradual charge loss.

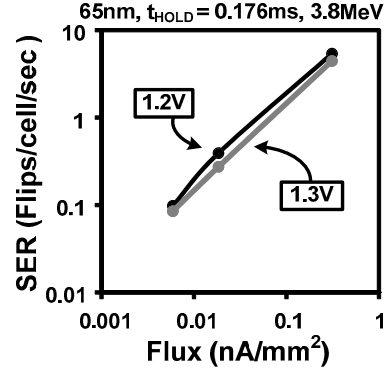


Fig. 9. Measured SER versus alpha particle flux.

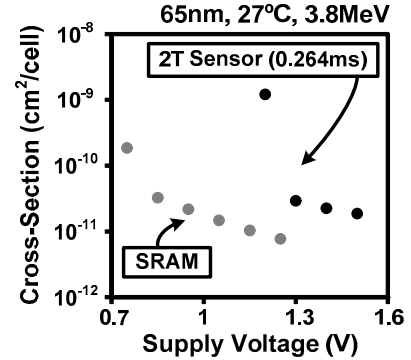


Fig. 10. Cross-section of 2T cell and SRAM measured at different supply voltages.

cells were tested under a lower supply voltage down to 0.75V. As shown in Fig. 10, the measured cross-section of the 2T sensor cell is $1.22\text{E-}9\text{ cm}^2/\text{cell}$ at 1.2V while a 6T SRAM has a cross-section of $1.04\text{E-}11\text{ cm}^2/\text{cell}$ at 1.15V for the same beam energy and radiation flux. This corresponds to a 117x higher cross-section area per cell for the 2T sensor as compared to a 6T SRAM.

IV. CRITICAL LET ANALYSIS

In this section, we compare the critical LET of the 2T structure, 6T SRAM cell and standard inverter chains for a better understanding of each circuit’s vulnerability to single event effects. A simple model has been used to evaluate the critical LET for different circuit topologies. A particle strike in the normal direction to the silicon chip induces a current pulse I_{rad} consisting of two parts:

$$I_{\text{rad}}(t) = I_{\text{substrate}}(t) + I_{\text{drain}}(t) \quad (2)$$

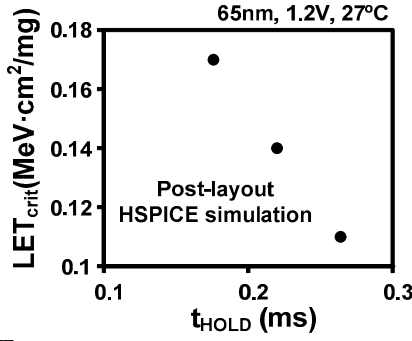


Fig. 11. LET_{crit} versus t_{HOLD} .

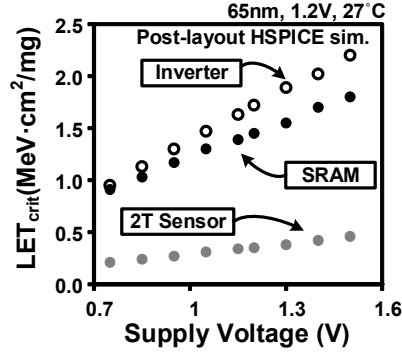


Fig. 12. Simulated LET_{crit} for inverter, 6T SRAM, and 2T sensor.

where I_{drain} and $I_{substrate}$ are the strike induced drain and substrate current, respectively.

(i) Substrate current $I_{substrate}$

The substrate current can be approximated using the double exponential empirical equation as follows:

$$I_{substrate}(t) = \frac{Q}{(\tau - 0.5\tau)} (e^{-t/\tau} - e^{-t/0.5\tau}) \quad (3)$$

Q here is the charge deposited along the penetration path. 0.5τ and τ are the fall time and rise time constants, respectively. These two parameters can be approximated as [4]:

$$Q = 10 \times LET \times d_s \quad (4)$$

where Q is expressed in fC, LET is expressed in $MeV \cdot cm^2/mg$, and the distance d_s is the distance from the drain to the center of the charge packet generated in the substrate, expressed in μm . By performing a Fourier analysis of the charge packet, it can be shown that the dominant fall time constant is:

$$\tau = \frac{4}{\pi^2} \frac{d_s^2}{D_a} \quad (5)$$

Where D_a is the ambipolar diffusivity given by:

$$D_a = \frac{2D_n D_p}{D_n + D_p} \quad (6)$$

Here, D_n is the electron diffusivity and D_p is the hole diffusivity. Substituting equations (4), (5) and (6) into equation (3), one can obtain the radiation induced current in the substrate.

(ii) Drain current I_{drain}

The particle induced drain current pulse can be calculated in a similar way given by:

$$I_{drain}(t) = \frac{0.5Q}{(\tau - 0.5\tau)} (e^{-t/\tau} - e^{-t/0.5\tau}) \quad (7)$$

The charge Q is multiplied by a factor of 0.5 as compared that in equation (3). This is because half of the charge deposited in the drain will be dissipated through the top drain contact, while the other half of the charge deposited at the bottom of the drain will be collected.

Based on the above equations, a current source was modeled in VerilogA. This current source was then instantiated in Spectre and connected to the sensitive nodes to run HSPICE simulations. The 2T sensor's SER dependence on t_{HOLD} was also captured through the simulation. As shown in Fig. 11, critical LET (LET_{crit}) decreases monotonically with a longer t_{HOLD} . The critical LETs for an inverter chain, a 6T SRAM and the proposed 2T sensor have been simulated and plotted in Fig. 12. Simulation results show that LET_{crit} of the proposed 2T sensor cell is 3.4x-4.2x and lower than that of an inverter chain or SRAM cell for supply voltages from 0.75V to 1.5V.

V. CONCLUSION

In this work, we propose a compact 2T sensor structure providing a considerably higher sensitivity to radiation strikes compared to conventional SRAM structures. The 2T sensor array was implemented in a 65nm bulk process and tested under an accelerated alpha particle irradiation environment to verify the higher cross section area. Simulation results shows that critical LET of the proposed 2T sensor cell is 3.4x-4.2x smaller than that of an inverter chain and SRAM cell.

ACKNOWLEDGEMENTS

This work was partially supported by the Defense Threat Reduction Agency under Basic Research Award No. HDTRA1-14-1-0042. The authors would like to thank Dr. Greg Haugstad at the Characterization Facility, University of Minnesota, for help with the radiation testing, and Prof. Ik-Joon Chang at Kyunghee University for suggestions regarding the radiation parameters.

REFERENCES

- [1] A. Dixit et al., "The impact of new technology on soft error rates," International Reliability Physics Symposium (IRPS), pp. 5B.4.1-5B.4.7, 2011.
- [2] S. Lee, et al., "Radiation-induced soft error rate analyses for 14 nm FinFET SRAM devices," International Reliability Physics Symposium (IRPS), pp. 4B.1.1-4B.1.4, 2015.42-1649, Aug. 2015.
- [3] J. Noh, et al., "Study of Soft Error Rate (SER) Sensitivity: Investigation of Upset Mechanisms by Comparative Simulation of FinFET and Planar MOSFET SRAMs," IEEE transactions on Nuclear Science, vol. 62, no. 4, pp. 1
- [4] "PSTAR and ASTAR Databases for Protons and Helium Ions" Available: <http://physics.nist.gov/PhysRefData/Star/Text/programs.html>.
- [5] D. E. Fulkerson, "An Engineering Model for Single-Event Effects and Soft Error Rates in Bulk CMOS," IEEE Transactions on Nuclear Science, vol. 58, no. 2, pp. 506-515, April 2011.